Amino-grafted Cu and Sc Metal-Organic Frameworks involved in the green synthesis of 2-amino-4*H*-chromenes. Mechanistic understanding

D. González-Rodal,[a] G. Turnes Palomino,[b*] C. Palomino Cabello[b] y E. Pérez-Mayoral[a*]

[a]Departamento de Química Inorgánica y Química Técnica, Universidad Nacional de Educación a Distancia, UNED, Facultad de Ciencias, Urbanización Monte Rozas, Avda. Esparta s/n Ctra. de Las Rozas al Escorial Km 5, , E-528232 Las Rozas – Madrid (Spain).

[b]Departamento de Química, Universidad de las Islas Baleares, Cra. de Valldemossa km 7.5, 07122 Palma de Mallorca (Spain)

Corresponding authors:

Elena Pérez-Mayoral; eperez@ccia.uned.es

Phone (+34) 91 398 9047; Fax (+34) 91 398 6697

G. Turnes Palomino; g.turnes@uib.es

Phone (+34) 971 173250; Fax (+34) 971 173426

Abstract

In this work, we report for the first time a new methodology for the eco-synthesis of 2-amino-4*H*-chromenes **1**, from salycilaldehydes and cyano compounds, under solvent-free and mild conditions, using amino-grafted MOFs as catalysts. The selected MOFs – commercial CuBTC and MIL-100(Sc) previously synthetized in our laboratories – can be easily functionalyzed with amines of different nature showing notable differences in their composition and textural properties. The total or partial functionalization of the metal centers in starting MOFs is strongly depending on the functionalization method used. Our results indicate that the catalytic performance is mainly conditioned by the type and concentration of basic sites, porosity of the samples barely showing any influence. The methodology herein reported could be considered as an environmental friendly alternative to the selective chromene synthesis, which allows to achieve high yields in relatively short reaction times (up to 90% over 1h), using notably small amounts of easily prepared catalysts.

Furthermore, our experiments in combination with theoretical calculations strongly suggest that free-amine groups in ethylenediamine (EN) functionalized catalysts can act either as individual catalytic sites, *e. g.* EN-M/CuBTC sample, in which all metal centers are functionalized with EN ligands and shows the highest concentration of basic catalytic sites, or acting in cooperation with the closest metal centers in samples partially functionalized, as in the case of EN/CuBTC sample.

Key words

Amino-grafted metal-organic-frameworks, heterogeneous catalysts, chromene derivatives, fine chemicals

Highlights

Amino-grafted MOFs are able to efficiently catalyze the chromene synthesis

Functionalization of selected MOF is strongly depending of the method used

Amine functions in MOF can be act as individual catalytic sites

A cooperation of amine groups with the nearest metal CUS probably takes place in partially functionalized samples

1. Introduction

Metal-Organic Frameworks (MOFs) are fascinating organic-inorganic hybrid materials applied to a great variety of research fields such as gas storage, sensing, catalysis and even drug delivery among others [1-3]. The wide diversity of both metal ions and multidentate organic ligands available to form these 3D nanoporous networks by coordination makes possible the synthesis of these materials on demand [4].

Regarding catalytic applications, MOFs are considered promising candidates for catalyzing liquid phase reactions because of their textural properties – high surface areas and pore volumes – as well as their high concentrations of active sites accurately located [5]. In recent years, MOFs have been extensively explored as catalysts in acid-base and redox reactions [6], CO_2 chemical transformations [7], H_2 production [8] and as multifunctional catalysts in synergistic catalysis and tandem reactions [9] but also in the production of fine chemicals [10,11] involving aldol-based reactions [12]. At this respect, we reported experimental and theoretical studies concerning the synthesis of quinolines via Friedländer reaction catalyzed by $Cu_3(BTC)_2$ [13-16]. Much more recently, commercial Basolites, particularly C300, F300 and Z1200, have been proposed by some of us as efficient porous catalytic active systems in the synthesis of important heterocyclic scaffolds such as quinoxalines [17].

Chromene derivatives [18] are an extremely versatile class of heterocycles which has acquired especial relevance due to their therapeutic properties such as antiviral, antiproliferative, antioxidant, antihistaminic and others [19, 20]. These heterocyclic compounds have been also recognized as antiapoptotic Bcl-2 proteins useful in cancer treatments to avoid the drug resistance [21,22], and for the treatment of schizophrenia [23] or Alzheimer disease [24].

Different catalysts involved in the synthesis of chromenes, particularly 2-amino-4*H*-chromenes, have been reported. Among the most traditional homogeneous ones stand out highly polluting organic amines [25] whereas molecular sieves [26], anion exchange resins such as Amberlyst A-

21 [27], doped hydrotalcites [28] and zirconium phosphate [29], have been reported as heterogeneous catalysts. Developed methodologies so far are mostly characterized by the use of large amounts of inorganic solids and solvents, during prolonged reaction times, also requiring tedious isolation and purification steps to obtain the reaction products. These features contribute to the production of wastes, such as solid residues and liquid efluents, highly polluting, and to increase the energy consumption. In this context, we have recently reported some new and environmental-friendly catalytic systems, useful in the multicomponent synthesis of 2-amino-4*H*-chromenes **1** (Scheme 1) comprising ionic liquids like imidazolium sulfonates [30], bifunctional mesoporous metallosilicates [31,32] and, much more recently, CaO-carbon materials, easily prepared from PET and natural limestone allowing the valorization of both PET residues and mineral sources, mesoporous hydrotalcite/SBA-15 and hydrotalcite/hydroxyapatite composites [33].

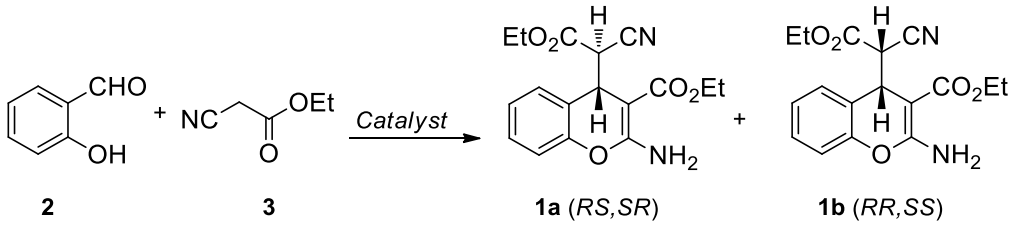

2 **3** **1a** (*RS,SR*) **1b** (*RR,SS*)

Scheme 1. Synthesis of 2-amino-4*H*-chromenes from salicylaldehyde **2** and ethyl cyanoacetate **3** under solvent-free conditions.

The goal of this work is the development of new MOF-derived catalysts with basic properties able to promote the synthesis of 2-amino-4*H*-chromene derivatives from salycilaldehydes and different nitriles. The existence of coordinatively unsaturated metal sites (CUS) in the selected MOFs allows the functionalization with organic amines by coordination using a post-synthetic approach, which is an usual strategy to modify the acid-base properties of these metal-organic networks. In this context, Hwang et al. reported the preparation of an amino-grafted MIL-101 and the evaluation of its catalytic behaviour in Knoevenagel condensation, between benzaldehyde and ethyl cyano acetate, resulting to show superior catalytic performance than

amino-grafted mesoporous silica APS-SBA-15 [34]. Based on that, and in order to study the influence of both basicity and textural properties on catalytic behaviour, we select two different MOFs – Basolite C300 (CuBTC) and MIL-100(Sc) –, in which metal ions Cu^{II} and Sc^{III}, respectively, are coordinated by trimesic acid (denoted as BTC) ligands, being both able to coordinate organic amines of distinct nature.

2. Materials and methods

The materials used in this research were commercially available. Chemical reagents and solvents were purchased from Sigma-Aldrich or Alfa-Aesar. Particularly, Basolite C300 was purchased from Sigma-Aldrich.

2.1. Synthesis of MIL-100(Sc)

MIL-100(Sc) was synthesized following the experimental procedure reported by Li et al [35]. Briefly, it was prepared by mixing $Sc(NO_3)_3 \cdot H_2O$ (0.61 g) and trimesic acid (0.25 g) in DMF (45 mL). The mixture was stirred at room temperature for 30 min and then introduced into a Teflon-lined autoclave (100 mL) at 423 K for 36 h. The product was filtered off, washed with DMF, and dried at room temperature.

2.2. Synthesis of amino-grafted MIL-100(Sc)

MIL-100(Sc) was functionalized following an adaptation of the experimental protocol reported by Hwang et al [34]. As-synthesized MIL-100(Sc) (1.0 g) was immersed in ethanol, at 373 K, for 20 h before being activated at 453 K for 12 h under nitrogen atmosphere to remove the terminal solvent molecules coordinated to the open metal sites. After activation, MIL-100(Sc) was suspended in anhydrous toluene (100 mL) and the corresponding amine (1.0 mL) was added. In order to make the grafting complete, the reaction mixture was refluxed under N_2 for 12 h. The resulting solid was washed with hexane to remove the unreacted amine, and dried at room temperature.

Two amino-grafted MIL-100(Sc) samples were prepared by using ethylenediamine (EN) or N,N'-dimethylethylenediamine (MMEN) denoted as EN-M/MIL-100(Sc) and MMEN-M/MIL-100(Sc), respectively.

2.3. Synthesis of amino-grafted CuBTC

Amino-grafted CuBTC samples were prepared by using two different methologies.

Method A: EN-M/CuBTC samples were prepared from CuBTC by reacting with EN following the experimental protocol described above and used for the functionalization of MIL-100(Sc).

Method B: For comparison purposes, analogous sample EN/CuBTC was prepared in the presence of diethyl ether as solvent [36]. Briefly, commercial CuBTC (0.6 g) was refluxed in diethyl ether (20 mL) with the corresponding amine (1.5 mmol) under vigorous stirring during 72 h. The obtained solid was washed with diethyl ether to remove the unreacted amine (5 x 5 mL) and dried at 323 K.

Following this method two amino-grafted CuBTC samples were then prepared by using ethylenediamine (EN) or diethylenetriamine (DET) denoted as EN/CuBTC and DET/CuBTC, respectively. In addition, we also prepared 2DET/CuBTC sample in which a double amount of DET was used.

2.4 Characterization of the catalysts

Textural parameters of the materials were determined from the N_2 adsorption/desorption isotherms obtained at 77 K with a TriStar II (Micromeritics) gas analyzer. The samples were previously outgassed at 413 K overnight. The data of the isotherms were analyzed by using the Brunauer-Emmett-Teller (BET) method to determine the specific surface area and the two dimensional non-local density functional theory (2D-NLDFT) model for the determination of pore volume and pore size distribution. Powder XRD data were collected using CuKα (λ = 1.5418 Å) radiation on a Bruker D8 Advance diffractometer. Fourier transform infrared (FTIR) spectra

were recorded using a Bruker Vertex 80v spectrometer equipped with an MCT cryodetector. For IR measurements, a thin, self-supported wafer of the samples was prepared and activated (outgassed) inside the IR cell under dynamic vacuum at 423 K for 6 h. After this activation treatment, carbon monoxide was dosed into the cell to study the coordinatively unsaturated metal centers. Elemental analyses of the solids were carried out with Elemental Analyser LECO CHNS-932. Catalysts copper content was determined by AES (Atomic Emission Spectroscopy), using a ICP-OES PlasmaQuant PQ 9000 (Analytik Jena) spectrometer.

2.5 Catalytic performance

In a typical experiment carried out at 323 K or 303 K, the catalyst (25 mg) was added to a mixture of salicylaldehyde **2** (2 mmol) and ethyl cyanoacetate **3** (4 mmol) and the reaction mixture was stirred during 3 h. The reactions were carried out in a multiexperiment work station Starfish, in liquid phase, under atmospheric pressure and solvent-free conditions. Samples of the reacting mixtures were periodically taken after certain times for analysis by Proton Nuclear Magnetic Resonance (^{1}H NMR) — 15, 30, 60, 120 and 180 min —. The samples were diluted with CH_2Cl_2 (1 mL) to facilitate the separation of the catalyst by filtering off using a glass syringe equipped with a microfilter (Millipore, 0.45 μm HV). Finally, the solvent was evaporated in vacuo.

The progress of the reactions was qualitatively monitored by thin layer chromatography (TLC) performed on a DC-Aulofolien/Kieselgel 60 F245 (Merck), using CH_2Cl_2/EtOH (98:2) mixture as an eluent.

The yield (or conversion) of the process is defined as the fraction of reactant **2** transformed at each reaction time into compounds, determined by ^{1}H NMR.

Reaction products were characterized by ^{1}H NMR spectroscopy. Solution NMR spectra were recorded on a Bruker DRX 400 (9.4 Tesla, 400.13 MHz for ^{1}H) spectrometer with a 5-mm inverse-detection H-X probe equipped with a z-gradient coil, at 300 K. Chemical shifts (δ in ppm) are

given from internal solvent, $CDCl_3$ 7.26 for ^1H. Spectroscopic data of 2-amino-4*H*-chromenes **1**, **6** and **7** are in good agreement with those previously reported [25, 30].

2.6. Computational methods

The calculations showed in this work were performed by using the Gaussian 09 software package [37], in gas phase, at 298 K. All the geometries were optimized using B3LYP hybrid functional [38,39] with 6-31G(d,p) basis set, this functional being a methodology used to study nanostructures [40]. The stationary points were characterized by means of harmonic vibrational frequency analysis. Thus, the transition structures were confirmed to be first-order saddle points. The imaginary frequency was inspected in each transition structures to ensure it represented the desired reaction coordinate. For key transition states the intrinsic reaction coordinate (IRC) was followed to ensure it connects the reactants and products [41].

3. Results and discussion

3.1. Characterization of the catalysts

Figure 1 shows the X-ray diffraction patterns of CuBTC and MIL-100(Sc) before and after amine grafting. The CuBTC and MIL-100(Sc) samples showed good crystallinity and all diffraction lines could be assigned to the corresponding structural types. After the grafing process, the almost unchanged powder X-ray diffraction patterns of the samples indicate the preservation of the MOFs structure, except in the case of the EN-M/CuBTC sample, in which a slight variation of crystallinity is observed.

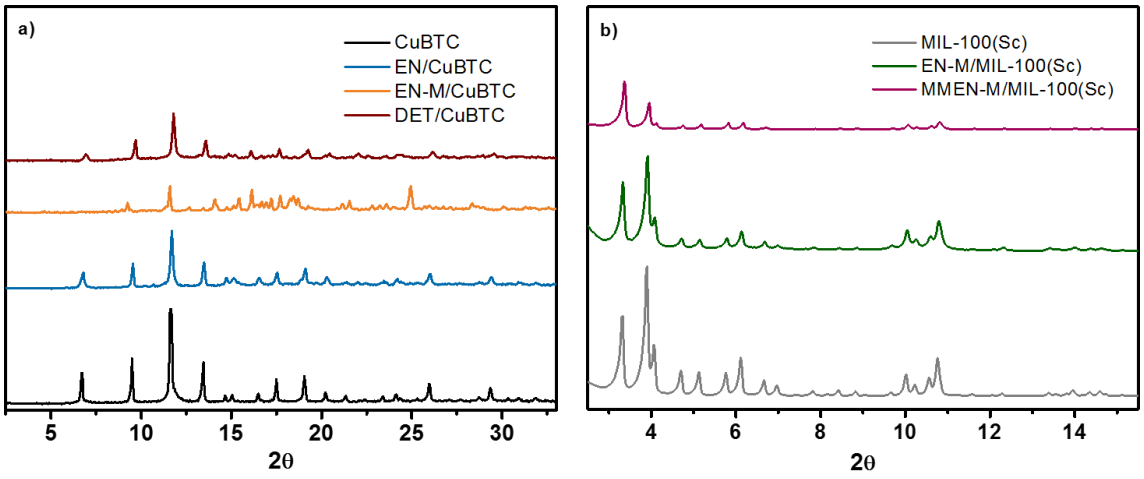

Figure 1. X-Ray diffractograms of amino-grafted a) CuBTC and b) MIl-100(Sc) samples.

Nitrogen adsorption-desorption isotherms were collected at 77 K for CuBTC (Figure 2a) and MIL-100(Sc) (Figure 2b) samples and were analyzed using the BET and 2D-NLDFT methods. The measured BET surface areas and pore volumes of bare MOFs (Table 1) are in agreement with previous results. Amine-grafted samples show a notable reduction of the specific surface area and pore volume, especially for MIL-100(Sc) samples, for which these parameters are 2 and 3 times lower than those of the bare sample (Table 1), indicating a partial occupation of the space inside the pores by the amine molecules. The particularly low value of the surface area of EN-M/CuBTC sample is probably due to the high amine loading reached in this case (see below). The pore size distributions (Figure S1) demonstrate the presence of micropores in CuBTC samples and a multimodal distribution in MIL-100(Sc) samples, and confirm the decreased porosity in the functionalized materials.

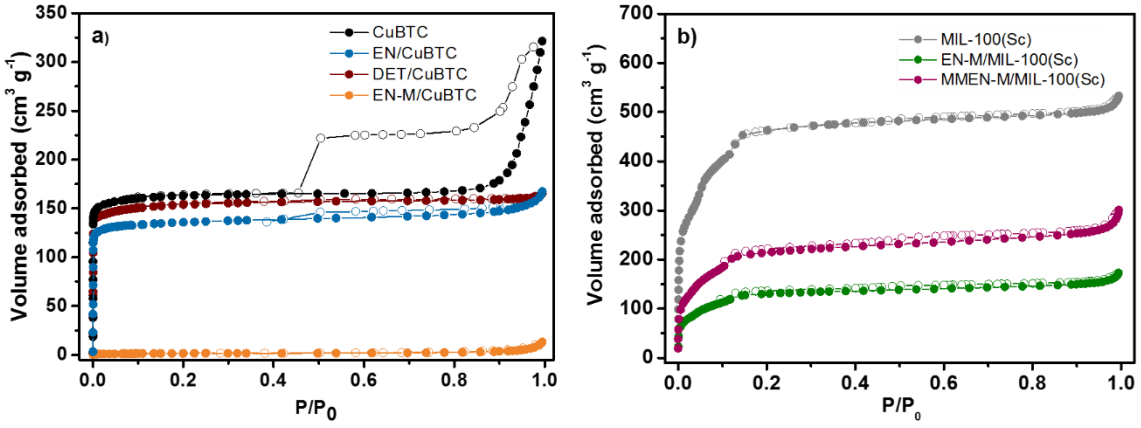

Figure 2. Nitrogen adsorption-desorption isotherms for amino-grafted a) CuBTC and b) MIL-100(Sc) samples.

Table 1. Catalyst textural properties.

Catalyst	S_{BET} (m^2 g^{-1})	V_p (cm^3 g^{-1})	Pore width (Å)
CuBTC	640	0.46	8.7
EN/CuBTC	546	0.23	9.3
DET/CuBTC	615	0.24	9.5
EN-M/CuBTC	6	0.016	-
MIL-100(Sc)	1590	0.72	10.9/16.7/19.9
EN-M/MIL-100(Sc)	444	0.23	10.8/16.7/19.0
MMEN-M/MIL-100(Sc)	736	0.41	10.4/16.7/19.0

The amine grafting of CuBTC and MIL-100(Sc) MOFs was also studied by FTIR spectroscopy. As shown in Figure 3, all the amine-grafted samples exhibit additional absorption bands in the range of 3450 to 2800 cm^{-1}, which are assigned to N–H and C–H stretching vibrations [42], confirming the incorporation of the amine molecules in the prepared samples. The functionalization with amine molecules on coordinatively unsaturated copper (CuBTC) and scandium (MIL-100(Sc)) cations was also checked by infrared spectroscopy of carbon monoxide adsorbed at 100 K. After the activation of the samples, a saturation dose of CO was introduced

into the IR cell and the corresponding spectra were recorded. The IR spectra of CO adsorbed on the bare MOFs (Figure 4) show an IR absorption band centred at 2170 cm^{-1} for CuBTC and 2183 cm^{-1} for MIL-100(Sc) that comes from the fundamental C–O stretching mode of carbon monoxide interacting (through the carbon atom) with the Cu^{II} and Sc^{III} cations, respectively [43]. Additionally, in the case of CuBTC, another IR band near 2128 cm^{-1} is observed, which, according to the literature, corresponds to the CO interacting with Cu^{I} species formed during the activation treatment of the sample [44]. The IR spectra of the EN/CuBTC and DET/CuBTC samples (Figure 4a) show the IR absorption band at 2170 cm^{-1}, although much less intense, indicating that the open copper sites in these samples are partially grafted by the amine molecules. In the case of the EN-M/CuBTC, the IR absorption band at 2170 cm^{-1} completely disappears (Figure 4a) which, together with the porosity results and compositional data, confirm the high incorporation of amine molecules in this sample. The spectra of the functionalized MIL-100(Sc) samples (Figure 4b) show that the band assigned to the CO stretching vibration of carbon monoxide adsorbed on Sc^{III} is not observed, indicating that in these samples, most of the metal centers are coordinated to the amine molecules.

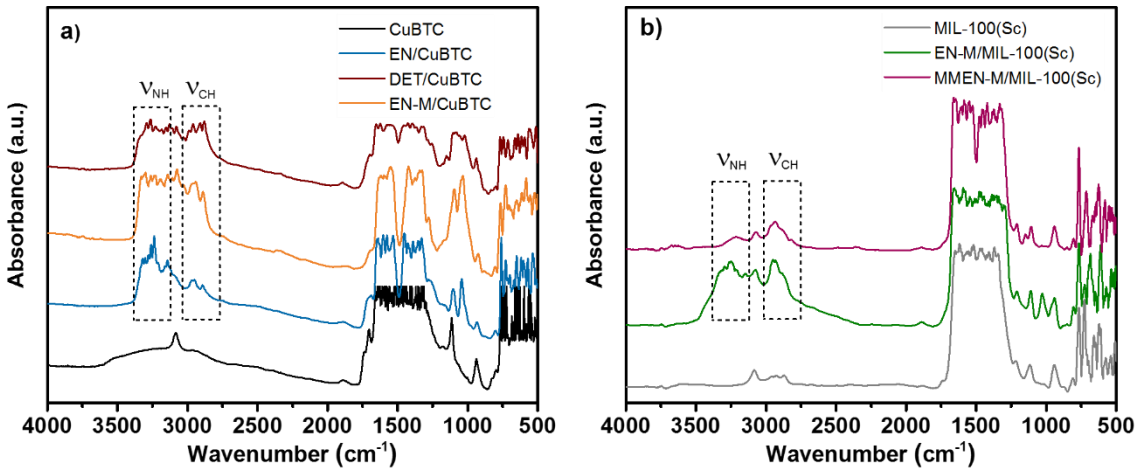

Figure 3. FTIR spectra for amino-grafted a) CuBTC and b) MIL-100(Sc) samples.

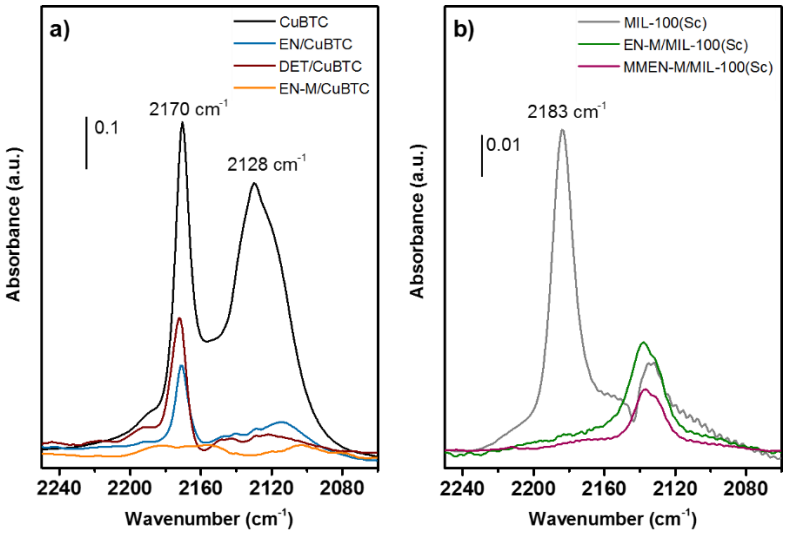

Figure 4. FTIR spectra of CO adsorbed at 100 K onbare and amino-grafted a) CuBTC and b) MIL-100(Sc) samples. IR absorption bands in 2240-2080 cm^{-1} region.

Considering these results, we also carried out elemental analysis of the prepared samples confirming the presence of N (Table 2). It can be observed remarkable differences between the synthesized catalysts depending on the method used for their functionalization. Assuming that only one $-NH_2$ group per amine molecule is coordinated to an unique metal atom in the MOF, EN/CuBTC and DET/CuBTC samples showed a N content considerably smaller than the Cu loading, which increases in the case of using a double amount of DET (2DET/CuBTC sample), although still remaining lower than the metal loading. However, in the case of EN-M/CuBTC, the N content is notably higher indicating that part of the EN molecules are coordinated to all available Cu atoms, while the rest are probably interacting with $-CO_2H$ defects present in the framework. Therefore, it can be affirmed that the functionalization of the MOFs under study with N-containing ligands strongly depends on the method used. Modification by using the method A produces the total saturation of metal CUS, while partially functionalized MOF samples are obtained when applying method B.

Table 2. Composition of the amino-grafted MOFs under study.

Sample	N[c] (mmol/g)	Cu[d] (mmol/g)
EN/CuBTC[a]	0,33	0,45
DET/CuBTC[a]	0,42	0,34
2DET/CuBTC[a]	0,58	0,31
EN-M/CuBTC[b]	1,20	0,29
EN-M/MIL-100(Sc)[b]	0,43	--
MMEN-M/MIL-100(Sc)[b]	0,30	--

Prepared by using the [a] method B, [b] method A.

Determined by [c] elemental anlysis and [d] ICP-OES.

3.2 Catalytic performance

The amino-grafted MOFs were tested in the synthesis of 2-amino-4*H*-chromenes **1**, from salicylaldehyde **2** and ethyl cyanoacetate **3**, under solvent-free conditions (Scheme 1). Firstly, for comparison, we explored the catalytic performance of the EN-grafted catalysts, at 323 K. It is important to remark that both supports, CuBTC and MIL-100(Sc), resulted totally inactive in this transformation even at high temperatures.

Figure 5 shows conversion values of salicylaldehyde **2** to chromenes **1** *vs* time in the presence of amino-grafted catalysts. It can be observed that the highest conversion values to chromenes **1** (up to 90 % after 2h), as mixtures of the corresponding diastereoisomers **1a**/**1b** in approximately 2:1 ratio, are obtained when using EN-M/CuBTC, the non-porous sample presenting the superior amount of EN ligand anchored to CuBTC, as confirmed by FTIR and elemental analysis (%N: 1.20 mmol/g) (Figure 5a). Considering that an unique -NH_2 function in EN ligand is coordinated to the corresponding metal center in CuBTC or MIL-100(Sc), as mentioned above, differences in the catalytic behaviour of EN-functionalized samples could be firstly attributed to the presence of

available catalytic active sites, comprising free -NH_2 functions groups (0.60, 0.17 and 0.22 mmol/g for EN-M/CuBTC, EN/CuBTC and EN-M/MIL-100(Sc) respectively, Table 2). Regarding the porosity of the catalysts, EN/CuBTC and EN-M/MIL-100(Sc) samples present similar V_p (0.23 $cm^3\ g^{-1}$), however EN/CuBTC sample shows larger S_{BET} (546 *vs* 444 $m^2\ g^{-1}$), which could be behind the slightly higher conversion values obtained at the shortest reaction times when using this sample (Figure 5a, Table 1). In the same context, EN-M/CuBTC and EN-M/MIL-100(Sc) catalysts are able to promote the reaction at lower reaction temperature; at 303 K, EN-M/CuBTC affords chromenes **1** in 91% of conversion, after 2h of reaction time, with maintained selectivity towards chromene **1a**, as thermodynamically stable isomer (Figure 5b). These results strongly suggest that free-amine functions in the investigated catalysts are the active specie promoting the reaction. In fact, EN/CuBTC sample with the lowest concentration of available amine groups resulted active in the chromene synthesis although reaching the lowest conversions (Figure 5a) (*see* computational section).

We also checked the catalytic behaviour of MOFs modified with amine of different nature, MMEN-M/MIL-100(Sc) and DET/CuBTC (Figure 5c and d). MMEN-M/MIL-100(Sc), having a similar concentration of N than DET/CuBTC, resulted active in the investigated transformation, at 323 K (Figure 5c), yielding the corresponding chromenes **1** in 82%, after 3h of reaction time, being the conversion values notably higher compared to those obtained for EN-M/MIL-100(Sc) (Figure 5a). Enhanced catalytic performance observed for MMEN-M/MIL-100(Sc) sample could be attributed to the presence of free secondary amine (–NH-CH_3) groups with increased basicity in comparison with primary amine function in EN ligand. In the same context, we also tested the DET/CuBTC catalyst, affording chromenes **1** in 78% in only 30 min of reaction time (Figure 5c). The same trend was observed when the reaction was carried out at 303 K observing the formation of chromenes **1** with lower conversion as expected (Figure 5d). These results indicate that the reaction is mainly controlled by the basicity of the samples. On the other hand, MMEN-M/MIL-100(Sc) shows superior S_{BET} (736 *vs* 615 $m^2\ g^{-1}$) and V_p (0.41 *vs* 0.24 $cm^3\ g^{-1}$) than

DET/CuBTC catalyst, therefore, in this case, texture of the catalysts does not seem to influence the catalytic performance.

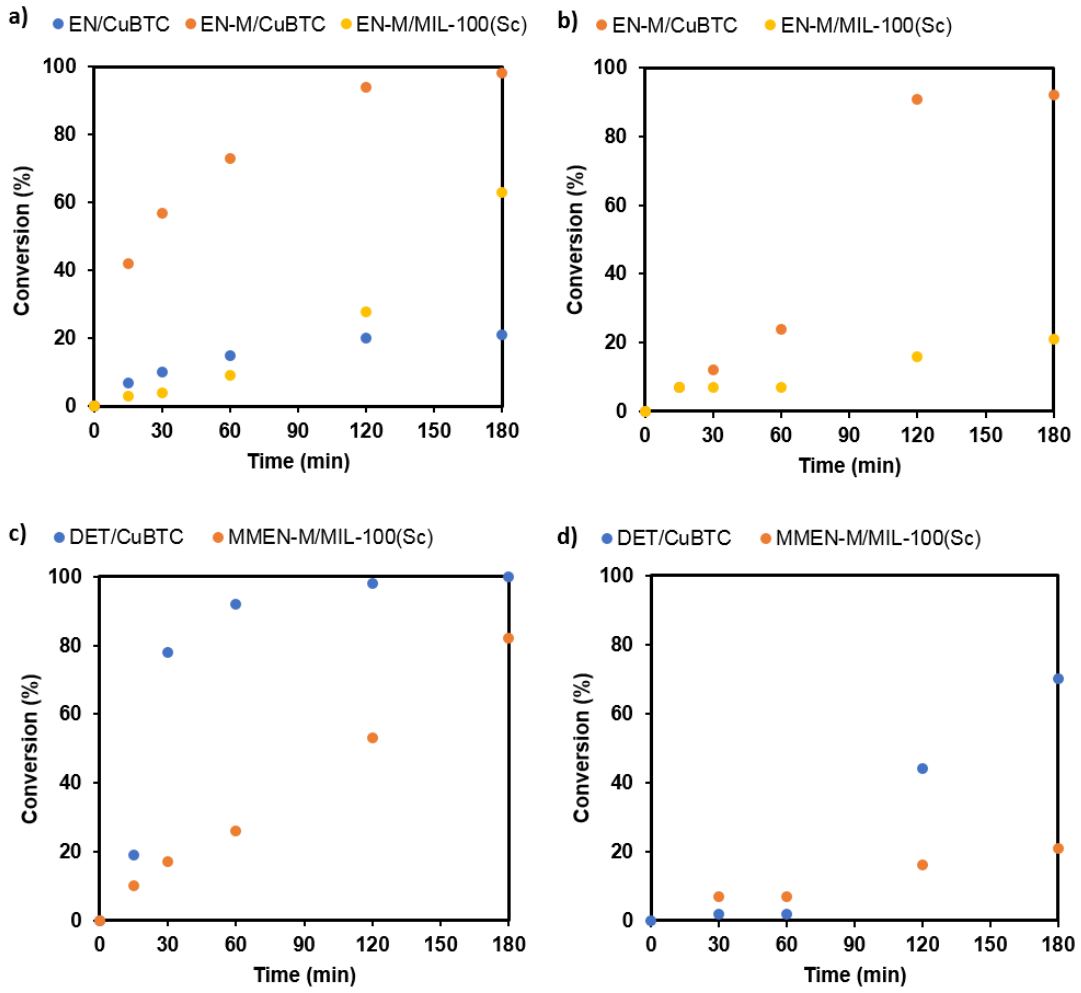

Figure 5. Synthesis of 2-amino-4*H*-chromenes **1**, from salicylaldehyde **2** and ethyl cyanoacetate **3**, under solvent-free conditions, catalyzed by a) amino-grafted CuBTC and MIL-100(Sc) at 323 K, b) EN-M/CuBTC EN-M/MIL-100(Sc) at 303 K, c) DET/CuBTC and MMEN-M/MIL-100(Sc) at 323 K and d) DET/CuBTC and MMEN-M/MIL-100(Sc) at 303 K.

Assuming the interaction of DET with Cu centers in CuBTC through one of the terminal $-NH_2$ groups [34], which are sterically less hindered, the secondary amine functions comprising the central N, substituted with ethylene bridges, in DET should be responsible of the observed reactivity. It is important to note that although the primary and secondary amine functions are

able to catalyze the reaction (Figure 5) and that DET/CuBTC shows the presence of both goups, it seems reasonable to think that both cannot independently and simultaneously work. In fact, taken into account that both samples, MMEN-M/MIL-100(Sc) and DET/CuBTC, show similar concentration of available secondary amine groups, additional factors should be behind the extraordinarly high conversion values to chromenes **1** observed when using DET/CuBTC catalyst (*see* computational section). 2DET/CuBTC sample presenting increased N loading showed a catalytic behaviour quite similar to DET/CuBTC.

Taken into account all these results, although $-NH_2$ functions in EN-M/CuBTC or EN-M/MIL-100(Sc) are able to catalyse the reaction yielding the corresponding chromene derivatives, acting as individual active sites, the presence of metal CUS sites in EN/CuBTC or DET/CUBTC could suggest that both samples can operate as bifunctional catalysts, in which amine functions and free-metal centers could be responsible of the nucleophile and electrophile activations. This hypothesis is especially relevant when comparing the conversion values observed in the presence of EN-M/CuBTC and DET/CuBTC catalysts; while the reaction catalyzed by EN-M/CuBTC, with the highest concentration of amine groups, led to chromene **1** in 57% after 30 min of reaction time, notably superior conversion values (78%, 30 min) were observed in the presence of DET/CuBTC sample.

The influence of the catalyst amount was explored in the reaction by using 2DET/CuBTC sample, observing an increase in conversion values to **1** from 14% (catalyst: 25 mg) to 82% (catalyst: 50 mg), after only 15 min of reaction time. The same trend was also observed when using other less active catalyst such as MMEN/MIL-100(Sc), affording chromenes **1** in 96% (50 mg of the catalyst) of conversion, after 3h of reaction time, compared to 82% (Figure 5c, 25 mg of the catalyst).

The scope of the methodology was investigated by using different substituted salycilaldehydes **4** but also other cyano compound such as malonitrile **5** (Table 3, scheme 2). In all the cases, chromenes **7** were selectively synthetized in good-to-excellent yields in the presence of amino-

grafted investigated MOFs. Particularly chromene **6** (R^1 = H and R^2 = CN) was obtained in quantitatively yield in the presence of EN-M/MIL-100(Sc) in only 15 min of reaction time under mild condition (303 K) (Table 3, entry 2). Even when using EN/CuBTC, the sample with minor concentration of $-NH_2$ functions, the corresponding chromene derivative was obtained in almost 90%, due to the strong reactivity of malononitrile **5** (Table 3 entry 1). Influence of substition at position 5- in the aromatic ring of salycilaldehydes **4** was investigated in the presence of the most active catalyst, DET/CuBTC, obtaining, in all the cases, the corresponding chromene derivatives **7** in good-to-excellent conversions (**7a**/**7b** 2:1 ratio) (Table 3, entries 3-6). The observed reactivity order is as follows: H ≈ NO_2 > Br > OMe. It seem then that the presence of electrowithdrawing substituents at position 5- in salyciladehyde favours the reaction. Based on our previous studies concerning the use of amino-grafted mesoporous silicas as catalysts involved in the synthesis of coumarins from salyciladehyde and ethyl acetoacetate [46], the substitution in salycilaldehyde affects not only to the electrophilicity of -CHO functions but also to the acidity of the *para* -OH group. Although the presence of electrodonating substituents on aromatic ring should favor the first step of the reaction comprising the aldolic reaction between reagents, electrowithdrawing substituents at position 5- produces an increment of acidity of phenol groups probably driving the heterocyclization step, since when R^1 is NO_2 group the reaction takes place even at lower temperatures affording mixtures of chromenes **7** with increased selectivity to **7a** (**7a**/**7b** 3:1 ratio).

Interestingly, ethyl 2-amino-6-bromo-4-(1-cyano-2-ethoxy-2-oxoethyl)-4*H*-chromene-3-carboxylate **7** (**HA 14-1**), where R^1 is Br and R^2 is CO2Et, as an agonist for Bcl-2 protein [21,22] which is expressed in most types of cancer, can be efficiently synthesized, as a diastereomeric mixture in a 2:1 ratio, in 90% of conversion after 3h of reaction time (Table 3, entry 4).

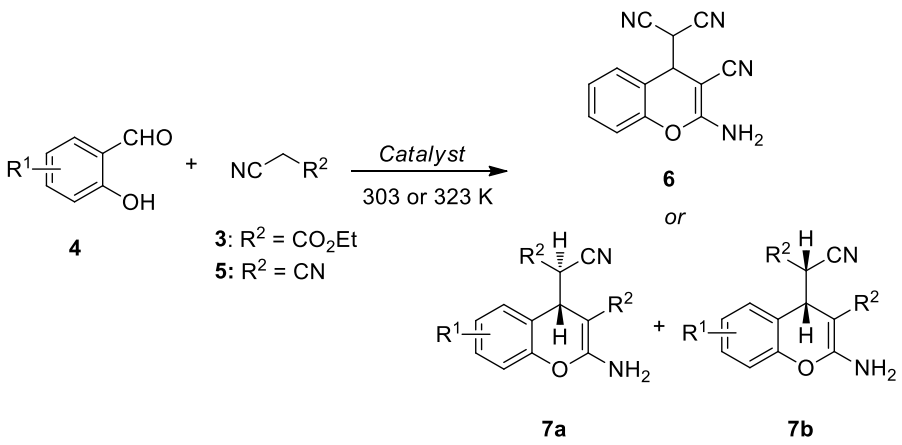

Scheme 2. Synthesis of chromenes **6** and **7** from salycilaldehydes and cyano compounds, at 303 or 323 K,under solvent-free conditions.

Table 3. Synthesis of chromenes **6** and **7** from salycilaldehydes and cyano compounds catalyzed by amino-grafted CuBTC.

Entry	**Catalyst**	**R^1**	**R^2**	**Temperature (K)**	**Time (min)**	**Conversion to 6 or 7(%)**
1	EN/CuBTC	H	CN	303	15	87
2	EN-M/MIL-100(Sc)	H	CN	303	15	99
3	DET/CuBTC	H	CO_2Et	323	60 (120)	92 (98)
4	DET/CuBTC	Br	CO_2Et	323	180	87
5	DET/CuBTC	OMe	CO_2Et	323	180	52
6	DET/CuBTC	NO_2	CO_2Et	323	60 (120)	84 (99)

Reaction conditions: Salycilaldehyde (2 mmol), cyano compound (4 mmol), catalyst (25 mg).

3.3. Computational study

In order to rationalize the obtained results, the aldolization reaction, as rate-limiting step in the synthesis of chromenes **1**, catalyzed by amino -grafted CuBTC, was theoretically analyzed. Considering previous studies concerning the Friedländer reaction catalyzed by CuBTC [15], reduced models representing CuBTC but also functionalized with the corresponding amines were selected (Figure 6). In these models it was observed a slightly increment of the Cu–Cu distance in amino-grafting catalysts regarding the bare CuBTC - 2.4746 Å (Figure 6a), 2.5575 Å (Figure 6b), 2.5570 (Figure 6c) – while the Cu–NH_2 distance maintained in approximately 2.146 Å.

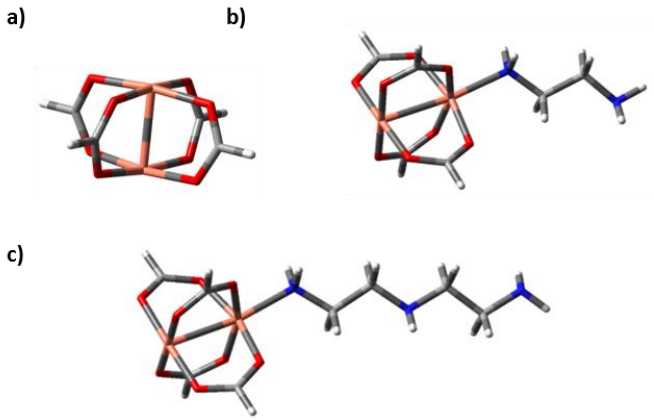

Figure 6. Reduced model simulating a) bare CuBTC, b) EN or EN-M/CuBTC and c) DET/CuBTC.

Since the reaction is catalyzed by basic species, as experimentally demonstrated, the transition structures for the uncatalyzed reaction or in the presence of bare CuBTC have not been investigated. Having in mind our previous studies analyzing amino-grafted mesoporous silicas [46,47], we explored the aldolization reaction between ethyl cyanoacetate **3** and salycilaldehyde **2**, in which compound **3** is able to donate a proton to amine functions in catalyst, through *keto* or *enol* forms, this proton subsequently activating the carbonyl acceptor, the -CHO group in compound **2**. Comparing both optimized transition structures when using the reduced model b or c (Figure 6) simulating EN/CuBTC (Figure 7a and 8a) and DET/CuBTC catalysts (Figure 7b and

8b), respectively, it can be observed, in both cases, a more advanced transition structures when ethyl cyanoacetate **3** is involved as enol form (Figure 8) as confirmed by computed C-C bond forming distances (2.1761 *vs* 2.5499 for EN/CuBTC catalyst and 2.1274 vs 2.6186 for DET/CuBTC catalyst). In the same context, the formation of TS-EN_B (*enol* form, Figure 8a) requires lower free energy barrier in 14.10 kcal/mol than TS-EN_A (*keto* form, Figure 7a) observing the same trend for TS-DET_B – 16.61 kcal/mol more stable than TS-DET_A (Figure 7a) –; this diminution is probably due to the stabilization of the TS by hydrogen bondings involving $-NH_2$ functions. Both observations suggested that ethyl cyanoacetate **3** reacts with salycilaldehyde **2** through its enol form (Figure 8). However, the small free energy differences do not justify the catalytic behavior observed for both EN/CuBTC and DET/CuBTC catalysts, probably indicating that additional factors could determine the catalytic performance.

Motivated because both catalysts, EN/CuBTC and DET/CuBTC, showed only a few Cu sites grafted with the corresponding amines, the computational and experimental results seems to suggest that amine functions and metal CUS in these catalysts could act in cooperation. Investigating this possibility we firstly analyzed the interaction modes of reactants with uncoordinated Cu centers using the reduced model showed in Figure 6a. As it can be observed from Table 4, the most stable optimized structures comprise the interaction between ethyl cyanoacetate **3** through lone pairs from C=O or C≡N functions with Cu centers showing slight free energy deviation.

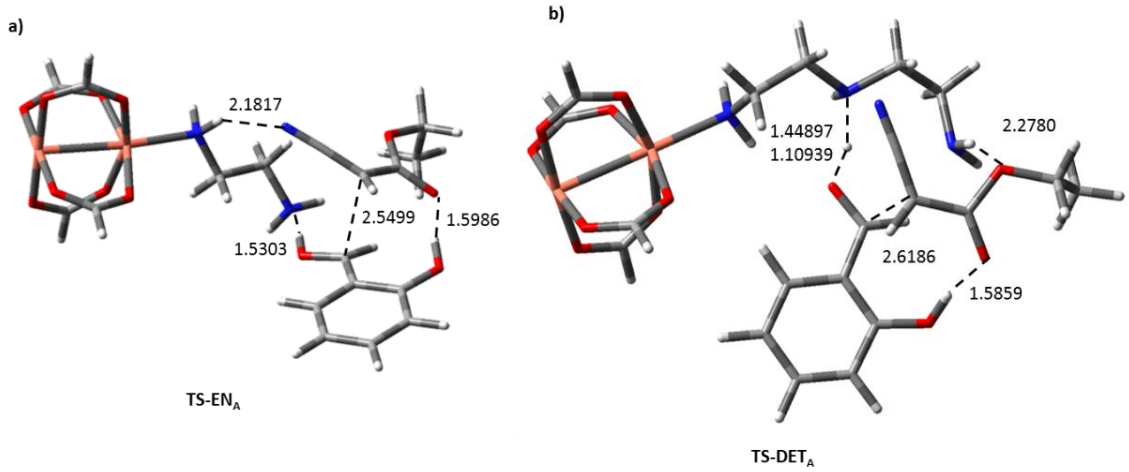

Figure 7. Optimized transition structures for the aldolization reaction between salycilaldehyde **2** and ethyl cyanoacetate **3** (*keto* form) catalyzed by a) EN/CuBTC and b) DET/CuBTC. Relevant distances are expressed in Å.

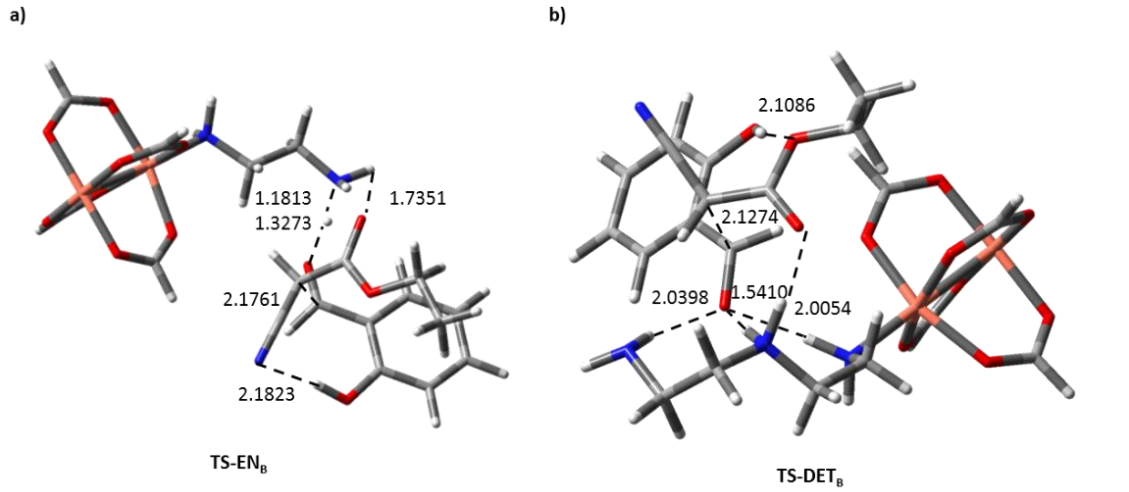

Figure 8. Optimized transition structures for the aldolization reaction between salycilaldehyde **2** and ethyl cyanoacetate **3** (*enol* form) catalyzed by a) EN/CuBTC and b) DET/CuBTC. Relevant distances are expressed in Å.

Table 4. Interactions of the reagents with metal centers in remaining metal CUS sites for amino-grafted CuBTC.

Interactions	**Compound**	**ΔG (Kcal/mol)**
Model a (Cu···O=C)	**2**	5,92
Model a (Cu···O-H)	**2**	9,04
Model a (Cu···O=C-O)	**3**	-1,08
Model a (Cu···N≡C)	**3**	-0,48
Model a (Cu···O-C=O)	**3**	3,21

In order to probe our hypothesis, we select an extended cluster simulating CuBTC in which one Cu atom is functionalized with amine groups of EN ligand whereas the closest Cu atom is interacting with ethyl cyanoacetate **3** through either C=O (Figure 9a) or C≡N groups (Figure 9b) as the most stable interactions. Briefly we used the most reduced models functionalizaed with EN molecules in order to reduce the computational cost. Slighly differences between both TS were observed concerning to C-C distances (2.5868 vs 2,5418 Å for TS-EN(Cu-CO) and TS-EN(Cu-C≡N) respectively) and free-energy barrier, TS-EN(Cu-C≡N) being 5 Kcal/mol more stable TS-EN(Cu-CO); these features make us to suspect that TS-EN(Cu-C≡N) is probably the operative TS. Considering these results and those previously obtained, the computed free energy value for TS-EN(Cu-CO) was aproximatley 10 kcal/mol lower compared to TS-EN_A (Figure 7a) showing similar interaction modes with the exception of -OH function now forming a strong hydrogen bonding with the CuBTC cluster. However, small free energy barrier, less than 1 kcal/mol, was observed when comparing TS-EN_B (Figure 7b) and TS-EN(Cu-C≡N) (Figure 9b), TS-EN_B being a more advanced transition structure as demonstrated by C-C bond forming distances (2.1761 vs 2.5418 Å for TS-EN_B and TS-EN(Cu-C≡N), respectively). Note that EN-M/CuBTC catalyst showed the absence of unsaturated Cu centers and, therefore, superior concentration of free $-NH_2$

functions (Table 2) able to promote the reaction, probably acting as individual catalytic sites throught TS-EN_B (Figure 8a), being this feature behind of its enhanced catalytic performance (Figure 5a). In the case of EN/CuBTC catalyst showing a low %Cu centers functionalized with amine groups, as experimentally demonstrated, the most probable transition structure could be TS-EN(Cu-C≡N), acting as bifunctional catalyst, in which the free amine function in EN could be able to abstract a proton of **3**, through its enol form, this proton activating the carbonyl acceptor in salycilaldehyde **2**, whereas -CN function is interacting with neightbouring unsaturated Cu centers. Thus, low conversion values of **2** obtained in the presence of EN/CuBTC sample could be attributed to a lower concentration of -NH_2 active centers in this catalyst but also to the interaction of ethyl cyanoacetate **3** through of C=O or C≡N functional groups with bare Cu centers, inhibiting the reaction with the time as experimentally observed (Figure 5a).

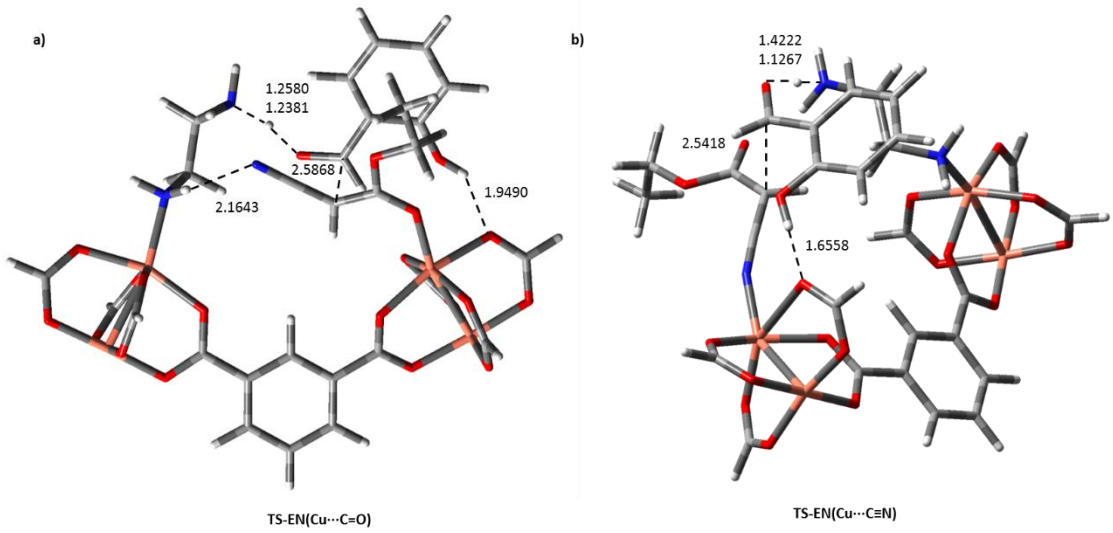

Figure 9. Optimized transition structure for the aldolization reaction between salycilaldehyde **2** and ethyl cyanoacetate **3** catalyzed by EN/CuBTC. a) Cu···O=C and b) Cu···N≡C interactions. Relevant distances are expressed in Å.

Considering these results, DET/CuBTC could act as bifunctional catalyst where ethyl cyanoacetate **3** would donate its acidic proton to secondary amine groups whereas simultaneously interacting with neighbouring CUS through –C≡N functions, –NH groups in each

amine groups participating in the activation of carbonyl acceptor in salycilaldehyde **2** as shown in TS-DET_B (Figure 8b). The presence of additional $-NH_2$ functions in this case should stabilize the corresponding TS, diminishing the free energy barrier as observed in TS-DET_B (Figure 8B).

4. Conclusions

We report herein for the first time a novel family of amino-grafted MOFs able to catalyze the the synthesis of 2-amino-4*H*-chromenes **1**, from salycilaldehydes and cyano compounds, under solvent-free and mild conditions. The catalysts were easily prepared by reacting the corresponding metal-organic network with organic amines, the functionalization of selected MOFs strongly depending of the used method. Our results demonstrate that the catalytic performance is mainly conditioned by the type and concentration of basic sites. It is supported by the catalytic behavior of EN-M/CuBTC and EN/CuBTC catalysts, being EN-M/CuBTC the most efficient catalyst, which shows high concentration of basic catalytic sites coordinating each metal centers in CuBTC. In the same context, the presence of secondary amine functions in DET/CuBTC or MMEN-M/MIL-100(Sc) samples favors the reaction. Since the porosity of the samples barely shows influence in catalytic performance, the reaction is then mainly controlled by the basicity of the samples.

Our experimental and theoretical results strongly suggest that available amine groups in EN functionalized catalysts can act either individual catalytic sites or in cooperation with the nearest CUS in samples partially functionalized; such is the case of EN-M/CuBTC and EN/CuBTC catalysts, respectively. In the case of using DET/CuBTC, the additional stabilization of the corresponding transition structure for the aldolization reaction, as the first elementary step in the formation of chromenes, involving strong hydrogen bondings NH···O=C and responsible of electrophile activation, could be behind of its superior catalytic performance.

5. Acknowledgments

This work has been supported by MICINN (Project CTM2014-5668-R).

6. References

[1] D. Farrusseng, S. Aguado, C. Pinel, Metal–organic frameworks: opportunities for catalysis, Angew. Chem. Int. Ed. 48 (2009) 7502-7513. https://doi.org/10.1002/anie.200806063.

[2] R.E. Morris, J. Čejka, Exploiting chemically selective weakness in solids as a route to new porous materials, Nat. Chem. 7 (2015) 381-388. https://doi.org/10.1038/nchem.2222.

[3] M. Almáši, V. Zeleňák, M. Opanasenko, J. Čejka, A novel nickel metal–organic framework with fluorite-like structure: gas adsorption properties and catalytic activity in Knoevenagel condensation, Dalton Trans. 43 (2014) 3730-3738. https://doi.org/10.1039/c3dt52698d.

[4] P. Z. Moghadam, A. Li, S. B. Wiggin, A. Tao, A. G. P. Maloney, P. A. Wood, S. C. Ward, D. Fairen-Jimenez, Development of a Cambridge Structural Database Subset: A Collection of Metal−Organic Frameworks for Past, Present, and Future, Chem. Mater. 29 (2017) 2618−2625. https://doi.org/10.1021/acs.chemmater.7b00441.

[5] J. Liang, Z. Liang, R. Zou, Y. Zhao, Heterogeneous Catalysis in Zeolites, Mesoporous Silica, and Metal-Organic Frameworks, Adv. Mater. 29 (2017), 1701139. https://doi.org/10.1002/adma.201701139.

[6] A. Dhakshinamoorthy, A. M. Asiric, H. Garcia, Catalysis by metal–organic frameworks in water, Chem. Commun. 50 (2014) 12800-12814. https://doi.org/10.1039/c4cc04387a.

[7] H. He, J. A. Perman, G. Zhu, S. Ma, Metal-Organic Frameworks for CO2 Chemical Transformations, Small 12 (2016) 6309-6324. https://doi.org.10.1002/smll.201602711.

[8] A. Rossin, G. Tuci, L. Luconi, G. Giambastiani, Metal–Organic Frameworks as Heterogeneous Catalysts in Hydrogen Production from Lightweight Inorganic Hydrides, ACS Catal. 7 (2017) 5035-5045. https://doi.org/10.1021/acscatal.7b01495.

[9] Y.-B. Huang, J. Liang, X.-S. Wang, R. Cao, Multifunctional metal–organic framework catalysts: synergistic catalysis and tandem reactions, Chem. Soc. Rev. 46 (2017) 126-157. https://doi.org/10.1039/c6cs00250a.

[10] M. Opanasenko, Catalytic behavior of metal-organic frameworks and zeolites: Rationalization and comparative analysis, Catal. Today 243 (2015) 2-9. https://doi.org/10.1016/j.cattod.2014.06.040.

[11] A. Dhakshinamoorthy, M. Opanasenko, J. Cejka, H. García, Metal organic frameworks as heterogeneous catalysts for the production of fine chemicals, Catal. Sci. Technol. 3 (2013) 2509-2540. https://doi.org/10.1039/c3cy00350g.

[12] A. Dhakshinamoorthy, M. Opanasenko, J. Cejka, H. Garcia, Metal Organic Frameworks as Solid Catalysts in Condensation Reactions of Carbonyl Groups, Adv. Synth. Catal. 355 (2013) 247-268. https://doi.org/10.1002/adsc.201200618.

[13] E. Pérez-Mayoral, J. Cejka, [Cu3(BTC)2]: A Metal–Organic Framework Catalyst for the Friedländer Reaction, ChemCatChem 3 (2011) 157-159. https://doi.org/10.1002/cctc.201000201.

[14] E. Pérez-Mayoral, Z. Musilová, B. Gil, B. Marszalek, M. Polozij, P. Nachtigall, J. Cejka, Synthesis of quinolines via Friedländer reaction catalyzed by CuBTC metal–organic-framework, Dalton Trans. 41 (2012) 4036-4044. https://doi.org/10.1039/C2DT11978A.

[15] M. Polozij, E. Pérez-Mayoral, J. Cejka, J. Hermann, P. Nachtigall, Theoretical investigation of the Friedländer reaction catalysed by CuBTC: Concerted effect of the adjacent Cu2+ sites, Catal. Today 204 (2013) 101-107. https://doi.org/10.1016/j.cattod.2012.08.025.

[16] M. Godino-Ojer, A. J. López-Peinado, F. J. Maldonado-Hódar, E. Pérez-Mayoral, Highly Efficient and Selective Catalytic Synthesis of Quinolines Involving Transition-Metal-Doped Carbon Aerogels, ChemCatChem 9 (2017) 1422-1428. https://doi.org/10.1002/cctc.201601657.

[17] M. Godino-Ojer, M. Shamzhy, J. Čejka, E. Pérez-Mayoral, Basolites: A type of Metal Organic Frameworks highly efficient in the one-pot synthesis of quinoxalines from α-hydroxy ketones under aerobic conditions, Catal. Today 345 (2019). https://doi.org/10.1016/j.cattod.2019.08.002.

[18] G. P. Ellis, The Chemistry of Heterociclic Compounds: Chromenes, Chromanones, and Chromones, John Wiley & Sons, Inc. , New York, 1977.

[19] W. P. Smith, L. S. Sollis, D. P. Howes, C. P. Cherry, D. I. Starkey, N. K. Cobley, Dihydropyranocarboxamides Related to Zanamivir: A New Series of Inhibitors of Influenza Virus Sialidases. 1. Discovery, Synthesis, Biological Activity and Structure- Activity Relationships of 4-Guanidino- and 4-Amino-4H-pyran-6-carboxamides, J. Med. Chem. 29 (1998) 787-797. https://doi.org/10.1021/jm970374b.

[20] A. Zonouzi, A. Mirzazadeh, M. Safavi, K.S. 0Ardestani, S. Emami, A. Foroumad, 2-amino-4-(nitroalkyl)-4H-chromene-3-carbonitriles as New Cytotoxic Agents, Int. J. Psychol. Res. 12 (2013) 679-685. https://doi.org/10.1021/jm970374b.

[21] W. Kemnitzer, J. Drewe, S. Jiang, H. Zhang, J. Zhao, C. Crogan-Grundy, L. Xu, S. Lamothe, H. Gourdeau, R. Denis, B. Tseng, S. Kasibhatla, S. Cai, Discovery of 4-Aryl-4-H-chromenes as a New Series of Apoptosis Inducers Using a Cell and Caspase-Based High Througput Screening Assay. 3. Structure- Activity Relationships of Fused Rings at the 7,8-Positions, J. Med. Chem. 50 (2003) 2858-2864. https://doi.org/10.1021/jm070216c.

[22] H. K. Keerthy, M. Garg, C. D. Mohan, V. Madan, D. Kanojia, R. Shobith, S. Nanjundaswamy, D. J. Mason, A. Bender, B. K. S. Rangappa, H. P. Kowffler, Synthesis and Characterization of Novel 2-Amino-Chromene-Nitriles that Target Bcl-2 in Acute Myeloid Leukemia Cell Lines, PLoS One, 9 (2014) 107-118. https://doi.org/10.1371/journal.pone.0107118.

[23] S. R. Kesten, T. G. Heffner, S. J. Johnson, T. A. Pugsley, J. L. Wright, D. L. Wise, Design, synthesis and evaluation of chromen-2-ones as potent and selective human dopamine D4 antagonists, J. Med. Chem. 42 (1999) 3718-3725. https://doi.org/10.1021/jm990266k.

[24] C. Bruhlmann, F. Ooms, P. Carrupt, B. Testa, M. Catto, F. Leonetti, C. Altomare, A. Cartti, A., Coumarins derivatives as dual inhibitors of acetylcholinesterase and monoamine oxidase, J. Med. Chem., 2001, 44, 3195-3198. https://doi.org/10.1021/jm010894d.

[25] M.A. Kulkarni, K. S. Pandit, U. V. Desai, U. P. Lad, P. P. Wadgaonkar, Diethylamine: A smart organocatalyst in eco-safe and diastereoselective synthesis of medicinally privileged 2-amino-4H-chromenes at ambient temperature, Comp. Rend. Chim. 16 (2013) 689-695. https://doi.org/10.1016/j.crci.2013.02.016.

[26] N. Yu, J. M. Aramini, M. W. Germann, Z. Huang, Reactions of salicylaldehydes with alkyl cyanoacetates on the surface of solid catalysts: syntheses of 4H-chromene derivatives, Tetrahedron Lett. 41 (2000), 6993-6996. https://doi.org/10.1016/S0040-4039(00)01195-3.

[27] J. S. Yadav, B. V. Subba Reddy, M. K. Gupta, I. Prathap, S. K. Pandey, Amberlyst A-21: An efficient, cost-effective and recyclable catalyst for the synthesis of unstituted 4h-chromenes, Catal. Commun. 8 (2007) 2208-2211. https://doi.org/10.1016/j.catcom.2007.05.005.

[28] U. Constantino, M. Curinir, F. Montanari, M. Nocchetti, O. Rosati, Hydrotalcite-like compounds as heterogeneous catalysts in liquid phase organic synthesis. II. Preparation of 4H-chromenes promoted by hydrotalcite doped with hydrous tin(IV) oxide, Micro. Meso. Mat. 107 (2008) 16-22. https://doi.org/10.1016/j.micromeso.2007.05.010.

[29] M. Curini, F. Epifano, S. Chimichi, F. Montanari, M. Nocchetti, O. Rosati, Potassium exchanged layered zirconium phosphate as catalyst in the preparation of 4H-chromenes, Tetrahedron Lett. 46 (2005) 3497-3499. https://doi.org/10.1016/j.tetlet.2005.03.075.

[30] J. Velasco, E. Pérez-Mayoral, V. Calvino-Casilda, A.J. López-Peinado, M.A. Bañares, E. Soriano, Imidazolium sulfonates as environmental-friendly catalytic systems for the synthesis of biologically active 2-amino-4H-chromenes: Mechanistic insights, J. Phys. Chem. B 119 (2015) 12042–12049. https://doi.org/10.1021/acs.jpcb.5b06275.

[31] A. Smuszkiewicz, J. López-Sanz, I. Sobczak, M. Ziolek, R. M. Martín-Aranda, E. Soriano, E. Pérez-Mayoral, Mesoporous niobiosilicate NbMCF modified with alkali metals in the synthesis of chromene derivatives, Catal. Today 277 (2016) 133–142. https://doi.org/10.1016/j.cattod.2016.02.042.

[32] A. Smuszkiewicz, J. López-Sanz, I. Sobczak, R. M. Martín-Aranda, M. Ziolek, E. Pérez-Mayoral, Tantalum vs Niobium MCF nanocatalysts in the green synthesis of chromene derivatives, Catal. Today 325 (2019) 47–52. https://doi.org/10.1016/j.cattod.2018.06.038.

[33] a) D. González-Rodal, J. Przepiórski, A.J. López Peinado, E. Pérez-Mayoral, Basic-carbon nanocatalysts in the efficient synthesis of chromene derivatives. Valorization of both PET residues and mineral sources, Chem Eng. J. 382 (2020) 122795. https://doi.org/10.1016/j.cej.2019.122795. b) F. D. Velazquez-Herrera, D. Gonzalez-Rodal, G. Fetter, E. Pérez-Mayoral, Enhanced catalytic performance of highly mesoporous hydrotalcite/SBA-15 composites involved in chromene multicomponent synthesis. Micropor. Mesopor. Mat. 309 (2020) 110569. https://doi.org/10.1016/j.micromeso.2020.110569. c) F. D. Velazquez-Herrera, D. Gonzalez-Rodal, G. Fetter, E. Pérez-Mayoral, Towards highly efficient hydrotalcite/hydroxyapatite composites as novel catalysts involved in eco-synthesis of chromene derivatives. Appl. Clay Sci. 198 (2020) 105833. https://doi.org/10.1016/j.clay.2020.105833.

[34] Y. K. Hwang, D. Y. Hong, J. S. Chang, S. H. Jhung, Y. K. Seo, J. Kim, A. Vimont, M. Daturi, C. Serre, G. Férey, Amine Grafting on Coordinatively Unsaturated Metal Centers of MOFs: Consequences for Catalysis and Metal Encapsulation, Angew. Chem. Int. Ed. 47 (2008) 4144 – 4148. https://doi.org/10.1002/anie.200705998.

[35] Y.T. Li, K. H. Cui, J. Li, J. Q. Zhu, X. Wang, Y. Q. Tian, The Giant Pore Metal-Organic Frameworks of Scandium Carboxylate with MIL-l00 and MIL-l01 Structures, Chin. J. Inorg. Chem. 27 (2011) 951-956.

[36] A. Das, M. Choucair, P. D. Southon, J. A. Mason, M.Zhao, C. J. Kepert, A. T. Harris, D. M. D'Alessandro, Application of the piperazine-grafted CuBTTri metal-organic framework in postcombustion carbon dioxide capture, Micro. Meso. Mat. 174 (2013) 74–80. https://doi.org/10.1016/j.micromeso.2013.02.036.

[37] M.J. Frisch, G.W. Trucks, H.B. Schlegel, G.E. Scuseria, M.A. Robb, J.R. Cheeseman, G. Scalmani, V. Barone, B. Mennucci, G.A. Petersson, H. Nakatsuji, M. Caricato, X. Li, H.P. Hratchian, A.F. Izmaylov, J. Bloino, G. Zheng, J.L. Sonnenberg, M. Hada, M. Ehara, K. Toyota, R. Fukuda, J. Hasegawa, M. Ishida, T. Nakajima, Y. Honda, O. Kitao, H. Nakai, T. Vreven, J.A. Montgomery, Jr., J.E. Peralta, F. Ogliaro, M. Bearpark, J.J. Heyd, E. Brothers, K.N. Kudin, V.N. Staroverov, R. Kobayashi, J. Normand, K. Raghavachari, A. Rendell, J.C. Burant, S.S. Iyengar, J. Tomasi, M. Cossi, N. Rega, J.M. Millam, M. Klene, J.E. Knox, J.B. Cross, V. Bakken, C. Adamo, J. Jaramillo, R. Gomperts, R.E. Stratmann, O. Yazyev, A.J. Austin, R. Cammi, C. Pomelli, J.W. Ochterski, R.L. Martin, K. Morokuma, V.G. Zakrzewski, G.A. Voth, P. Salvador, J.J. Dannenberg, S. Dapprich, A.D. Daniels, Ö. Farkas, J.B. Foresman, J.V. Ortiz, J. Cioslowski, D.J. Fox, Gaussian 09, Revision B.1., Gaussian, Inc., Wallingford CT, 2009.

[38] A. D. Becke, Density-functional thermochemistry. III. The role of exact exchange, J. Chem. Phys. 98 (1993) 5648–5652. https://doi.org/10.1063/1.464913.

[39] C. Lee, W. Yang, R.G. Parr, Development of the Colle-Salvetti correlation-energy formula into a functional of the electron density, Phys. Rev. B 37 (1988) 785–789. https://doi.org/10.1103/PhysRevB.37.785.

[40] N. R. Dhumal, M. P. Singh, J. A. Anderson, J. Kiefer, H. J. Kim, Molecular Interactions of a Cu-Based Metal−Organic Framework with a Confined Imidazolium-Based Ionic Liquid: A Combined Density Functional Theory and Experimental Vibrational Spectroscopy Study, J. Phys. Chem. C 120 (2016) 3295−3304. https://doi.org/10.1021/acs.jpcc.5b10123.

[41] C. Gonzalez, H.B. Schlegel, Reaction path following in mass-weighted internal coordinates, J. Phys. Chem. 94 (1990) 5523–5527. https://doi.org/10.1021/j100377a021.

[42] P. J. Harlick, A. Sayari, Applications of pore-expanded mesoporous silica. 5. Triamine grafted material with exceptional CO2 dynamic and equilibrium adsorption performance, Ind. Eng. Chem. Res. 46 (2007) 446-458.

[43] C. O. Areán, C. P. Cabello, G. T. Palomino, Infrared spectroscopic and thermodynamic study on hydrogen adsorption on the metal organic framework MIL-100(Sc), Chem. Phys. Lett. 521 (2012) 104–106. https://doi.org/10.1016/j.cplett.2011.11.054.

[44] J. Szanyi, M. Daturi, G. Clet, D. R. Baer, C. H. F. Peden, Well-studied Cu–BTC still serves surprises: evidence for facile Cu2+/Cu+ interchange, Phys. Chem. Chem. Phys. 14 (2012) 4383. https://doi.org/10.1039/C2CP23708C.

[46] N. Aider, A. Smuszkiewicz, E. Pérez-Mayoral, E. Soriano, R. M. Martín-Aranda, D. Halliche, S. Menad, Amino-grafted SBA-15 material as dual acid–base catalyst for the synthesis of coumarin derivatives, Catal. Today 227 (2014) 215–222. https://doi.org/10.1016/j.cattod.2013.10.016.

[47] A. Smuszkiewicz, E. Pérez-Mayoral, E. Soriano, I. Sobczak, M. Ziolek, R. M. Martín-Aranda, A. J. López-Peinado, Bifunctional mesoporous MCF materials as catalysts in the Friedländer condensation, Catal. Today 218– 219 (2013) 70– 75. https://doi.org/10.1016/j.cattod.2013.04.034.

Graphical Abstract